

**TERTIARY HALO AND TERTIARY BACKGROUND
IN THE LOW LUMINOSITY EXPERIMENTAL INSERTION IR8 OF THE LHC**

R.Assmann¹, D.Macina², K.M.Potter², S.Redaeli¹, G.Robert-Demolaize¹,
V.Talanov³ and E.Tsesmelis¹

Abstract

In our report we present the results for numerical simulation of tertiary halo and tertiary background in the LHC. We study the case of the proton losses in the betatron cleaning insertion IR7 with the subsequent tertiary halo generation in the downstream experimental insertion IR8. We analyze the formation of tertiary background in the experimental area of the IR8 and evaluate the performance of the machine-detector interface shielding with respect to this source of the background. The results obtained are compared with the previous estimates of the machine-induced background in the low luminosity insertions of the LHC, and the balance between different sources of the background is discussed.

¹ AB Division, CERN, Geneva, Switzerland

² TS Division, CERN, Geneva, Switzerland

³ TS Division, CERN, Geneva, Switzerland (on leave from IHEP, Protvino, Russia)

Presented at the Tenth European Particle Accelerator Conference (EPAC 2006)
26-30 June 2006, Edinburgh, United Kingdom

TERTIARY HALO AND TERTIARY BACKGROUND IN THE LOW LUMINOSITY EXPERIMENTAL INSERTION IR8 OF THE LHC

V. Talanov*, IHEP, Protvino, Russia, R. Assmann, D. Macina, K.M. Potter, S. Redaelli, G. Robert-Demolaize, E. Tsesmelis, CERN, Geneva, Switzerland

Abstract

In our report we present the results for numerical simulation of tertiary halo and tertiary background in the LHC. We study the case of the proton losses in the betatron cleaning insertion IR7 with the subsequent tertiary halo generation in the downstream experimental insertion IR8. We analyze the formation of tertiary background in the experimental area of the IR8 and evaluate the performance of the machine-detector interface shielding with respect to this source of the background. The results obtained are compared with the previous estimates of the machine-induced background in the low luminosity insertions of the LHC, and the balance between different sources of the background is discussed.

TERTIARY HALO AND TERTIARY BACKGROUND IN IR8

Fluxes of particles that reach the zones of the experiments on colliding beams form *machine induced background* which can be initiated within the machine by several sources. One source of the background of this type is *cleaning inefficiency* when the particles of the beam halo are scattered, but not absorbed, at primary and secondary collimators. These particles form the *tertiary halo* that escapes the cleaning insertion of the machine and is lost on the limiting apertures downstream along the ring. If the loss point of the halo is close to the experimental zone and the rate of these losses is significant then the resulting *tertiary background* can give a visible contribution to the total background level in the experiment.

The Large Hadron Collider at CERN [1] includes two cleaning insertions, betatron cleaning in the insertion region IR7 and momentum cleaning in IR3. We consider below the primary losses at the collimators in IR7 and subsequent losses of tertiary halo downstream from IR7 in the direction of Beam 1. We estimate the IR7 cleaning inefficiency and the rate of losses in the experimental insertion IR8 which is the closest aperture limitation to IR7 in the chosen beam direction. Taking these tertiary losses as the input source, we simulate secondary cascades in the mechanical and magnetic structure of IR8 to estimate the tertiary background at the entrance to the experimental zone of IP8.

The design of the LHC collimation system includes 16 tertiary collimators in pairs at each side of the experimental insertion, to provide machine protection and enhance

cleaning functionality for the tertiary halo [2]. Two of these collimators, as shown in Figure 1, will be installed at the IR7 side of IR8: the horizontal collimator TCTH at $(-118.688-117.208)$ m (close to the separation dipole D2) and the vertical TCTV at $(-74.23-72.75)$ m from IP8. Both collimators will have 1 m long tungsten (at the beam area) jaws with the cross-section of 80×25 mm. The opening of these collimators will be set to become the aperture restriction in the insertion and to collect most of the tertiary halo, protecting the superconducting magnets Q1-Q3 of the inner triplet from quenching.

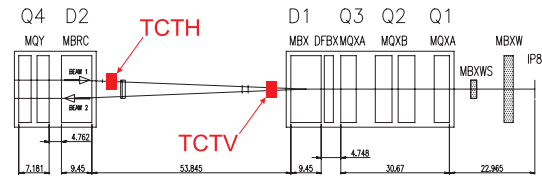


Figure 1: Layout of two tertiary collimators at the IR7 side of IR8: horizontal TCTH at D2 and vertical TCTV at D1.

SIMULATION OF CLEANING INEFFICIENCY

Detailed simulations of the loss distribution around the LHC ring and cleaning inefficiency were performed within the Collimation Project [3]. These calculations were done for nominal beam parameters and LHC collision optics with β^* of 10 m in IP8 and assumed an ideal cleaning. The settings of the main collimator families were 6σ for the primary and 7σ for the secondary collimators in IR7 and 8.3σ for the tertiary collimators in IR8. Calculations started with the simulation of the primary particle impact on the collimators in IR7 followed by the multi-turn tracking of the out-scattered particles through the machine lattice until the point of their loss.

Primary vertical and horizontal halos in IR7 were simulated separately. The results of the cleaning inefficiency calculations for vertical halo are given in Figure 2. Most of the losses in cold and warm LHC sections and also on the collimators are concentrated in IR7. Besides these, the green peaks on Figure 2 indicate the rate of the losses due to tertiary halo at the locations of tertiary collimators around experimental insertions. In total the calculations included $N_p \sim 5.01 \times 10^6$ particles scattered at the primary collimators in IR7. The number of them which were then lost at the TCTV/H in IR8 is given in Table 1. The absolute value for the loss rate can be obtained from these numbers by scaling

* Vadim.Talanov@ihep.ru

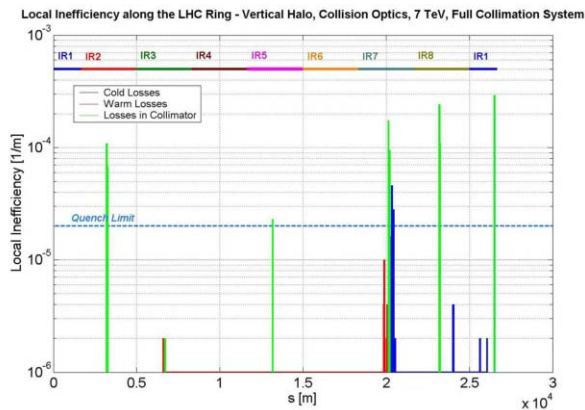


Figure 2: Loss distribution around the ring for betatron cleaning in IR7. The losses are expressed in terms of local cleaning inefficiency and are compared with the estimated quench limit for nominal intensity.

through a proportion where R_p is the rate of the losses on primary collimators for any given beam lifetime:

$$R_{(v,h)} = R_p \times \frac{N_{(v,h)}}{N_p}$$

Taking R_p for 30h beam lifetime equal to 2.8×10^9 protons/s according to [4] this gives the absolute rate $R_{(v,h)}$ of 2.35×10^6 and 0.61×10^6 protons/s, for losses at TCTV/H respectively. It is noted that the TCT settings are tighter than required for a β^* of 10m. The gaps can be and likely will be set to larger values. The results presented in this paper are conservative and will likely be lower with larger gaps.

Table 1: Number of particles $N_{(v,h)}$ lost at TCTV/H in the two separate simulations of different halo types.

Type of halo	N_v	N_h
Vertical	4195	1095
Horizontal	17	1509

ESTIMATION OF TERTIARY BACKGROUND

Simulation of tertiary background resulting from the losses on the collimators in IR8 was performed using the methodical approach developed for the solution of radiation problems at LHC [5]. Interactions of beam halo particles with the material of the collimator jaws were simulated according to particle characteristics recorded at TCTV/H in the tertiary halo calculations. Resulting secondary cascades were transported to the scoring plane at 1 m from IP8 where particle trajectories were stopped and analyzed. The threshold of 20 MeV on kinetic energy was applied in the simulation of transport for all particle types. Only the losses from vertical halo were simulated — as seen from Table 1 this type of halo gives the maximal loss rate.

Results of these secondary cascade simulations were the distributions of particle flux density at the entrance to the experimental zone of IP8 for different particle types. The distributions for charged hadrons and muons for the losses at TCTV are given at plots 1 and 3 in Figure 4 as $f(x, y)$ over the cross-section of the tunnel. Since TCTV is located close to the magnet line of D1-Q1, distributions for both particle types are featured by the clear shadow up to ~ 1 m from the beam line which represents the suppression of secondary particle fluxes by the material of the magnets. The muon distribution also shows spreading of particle flux in the horizontal plane by the field of the D1 dipole.

Total values for particle fluxes are given in column 2 and 4 of Table 2. Rates of tertiary background from TCTH were estimated to be of factor $\sim 40 \div 80$ lower than for TCTV due to the lower initial rate of the losses at the horizontal collimator and its more distant location from the position of the scoring plane.

Table 2: Particle flux, [particles/s] at 1 m from IP8, initiated by the losses from vertical halo at TCTV/H without (columns 2, 4) and with (columns 3, 5) shielding in IR8.

	Charged hadrons		Muons	
TCTV	5.7×10^6	5.8×10^4	1.7×10^6	4.9×10^5
TCTH	8.3×10^4	10^3	4.7×10^4	2.1×10^4
TOTAL	5.8×10^6	5.9×10^4	1.8×10^6	5.1×10^5

EVALUATION OF THE IR8 SHIELDING

Collisions in IP8 are foreseen at a nominal luminosity of $10^{32} \text{ cm}^{-2}/\text{s}$ which is significantly lower than in the high luminosity insertions IR1 and 5. At that luminosity there is no need of the TAS absorber in front of Q1 in IR8 to protect the inner triplet from the radiation from the interaction point. So at the tunnel entrance to the experimental zone there is no forward/inner shielding from the TAS which at IP1 and 5 not only protects outer detectors of the experiments from the scattered radiation from the TAS-Q1

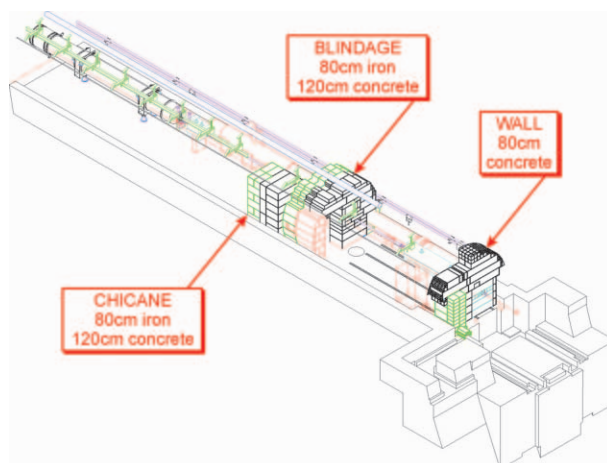


Figure 3: Layout of the shielding at the IR7 side of IR8.

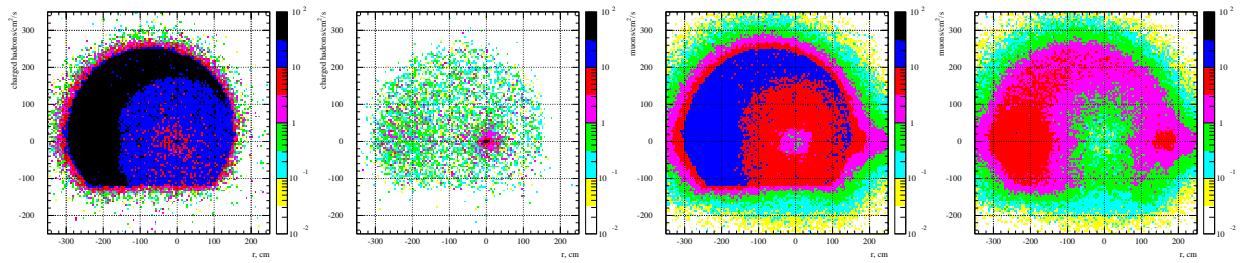


Figure 4: Particle flux density within the tunnel cross-section at 1 m from IP8, for charged hadrons and muons, without (plot 1 and 3) and with (2 and 4) the shielding at the IR7 side of IR8, for the losses at TCTV only.

region but because of its location also suppresses machine background that comes from the tunnel [6].

Due to mechanical constraints machine background shielding in IR8 has to be located in the machine tunnel around the vacuum chamber or magnet cryostat. Such shielding was proposed for IR8 and some shielding options were evaluated [7]. The final design of the full shielding configuration at the IR7 side of IR8, which consists of three concrete and iron plugs, is shown in Figure 3. The full configuration of this shielding which will be installed in IR8 for the nominal machine operation was introduced in the model of secondary cascade simulation and the results obtained were compared to those without the shielding.

Corresponding distributions for charged hadrons and muons over the cross-section of the tunnel are given at plots 2 and 4 in Figure 4. Total values for particle fluxes with the shielding in IR8 are given in column 3 and 5 of Table 2. For charged hadrons introduction of the shielding effectively suppresses this background component by two orders of magnitude, leaving only the fraction of the flux at the beam line around machine vacuum chamber. For muons the shielding removes $\sim 70\%$ of the total particle number, decreasing the flux of muons uniformly at the tunnel cross-section.

CONCLUSION

The estimates of tertiary background can be compared with previous ones for the background from beam-gas losses in IR8 from [7] and for the case of no shielding around IP8. Radial distributions of the background flux from these two sources are given in Figure 5. The source of tertiary background are localized losses in IR8 and the distributions for both charged hadrons and muons from TCTV/H without the shielding are flat with tertiary background dominating at high radii. Presence of the shielding removes the charged hadron flux everywhere but around the beam making it more than 10 times lower than that from the beam-gas losses. Muon flux even with the shielding overcomes the same beam-gas background component at the distance larger than ~ 1 m from the beam. If the beam lifetime is lower than the assumed 30 h with higher rates of losses in IR7, then the muon component of tertiary background will become the dominant part of the machine induced background in IR8.

REFERENCES

- [1] O. Brüning, P. Collier, P. Lebrun *et al.* (editors), “LHC Design Report. Volume I The LHC Main Ring”, CERN 2004-003, Geneva, 2004.
- [2] R. Assmann, C. Fischer, D. Macina *et al.*, “Integration of Tertiary Collimators, Beam-Beam Rate Monitors and Space Reservation for a Calorimeter in the Experimental LSS’s”, LHC Project Document LJ-EC-0003, CERN, Geneva, 2004.
- [3] R. Assmann, S. Redaelli, G. Robert-Demolaize, “LHC Collimation System Studies Using SIXTRACK”, Machine Induced Background Working Group meeting, CERN, Geneva, October 2005, <http://cern.ch/lhc-background>.
- [4] R. Assmann, “Collimators and Cleaning: Could This Limit The LHC Performance ?” In: Proc. of the LHC Performance Workshop — Chamonix XII, 2003, p.163–170.
- [5] I. Azhgirey, I. Baishev, K.M. Potter *et al.*, “Methodical Study of the Machine Induced Background Formation in the IR8 of LHC”, LHC Project Note 258, CERN, Geneva, 2001.
- [6] M. Huhtinen, N.V. Mokhov, “Machine Background in CMS. Status Report of Simulation Studies”, Machine Induced Background Working Group meeting, CERN, Geneva, March 2006, <http://cern.ch/lhc-background>.
- [7] I. Azhgirey, I. Baishev, K.M. Potter *et al.*, “Evaluation of Some Options for Shielding from Machine Induced Background in the IR8”, LHC Project Note 307, CERN, Geneva, 2002.

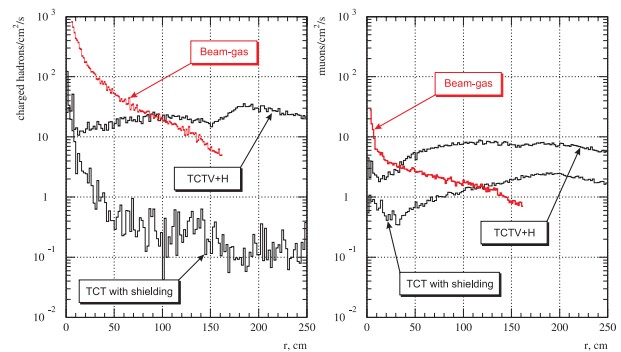


Figure 5: Particle flux density, [particles/cm²/s] at 1 m from IP8, calculated for the losses in TCTV/H without and with shielding in IR8, in comparison with the background from the beam-gas losses in IR8 with no shielding.